First observations of speed of light tracks by a fluorescence detector looking down on the atmosphere

(Article begins on next page)

04 July 2024

First observations of speed of light tracks by a fluorescence detector looking down on the atmosphere

Full author list for the JEM-EUSO collaboration

E-mail: `jeser@mines.edu`

ABSTRACT: EUSO-Balloon is a pathfinder mission for the Extreme Universe Space Observatory onboard the Japanese Experiment Module (JEM-EUSO). It was launched on the night(moonless) of the 24th of August 2014 from Timmins, Canada. The flight ended successfully after maintaining the target altitude of 38 km for five hours. One part of the mission was a 2.5 hour underflight using a helicopter equipped with three UV light sources (LED, Xe-Flasher, laser) to perform an inflight calibration and examine the detectors capability to measure tracks moving at the speed of light. We describe the helicopter laser system and details of the underflight as well as how the laser tracks where recorded and found in the data. These are the first recorded laser tracks measured from a fluorescence detector looking down on the atmosphere. Finally we present a first reconstruction of the direction of the laser tracks relative to the detector.

KEYWORDS: cosmic ray; JEM-EUSO; EUSO-Balloon; prototype; test beam; laser; helicopter; stratospheric balloon;.

Contents

1. Introduction

To measure extreme energetic cosmic with high statistics a large observation area is needed. One options is to go to space. JEM-EUSO (Extreme Universe Space Observatory on board the Japanese Experiment Module) is a planned fluorescence detector on the International Space Station [1]. It is designed to measure the light of extensive air showers developing in the Earth's atmosphere beneath the detector. Further space instruments in the design stage are KLYPHE-EUSO and POEMMA [2, 3]. Various prototypes are developed for the JEM-EUSO mission [4, 5, 6]. The first one is EUSO-Balloon.

The EUSO-balloon mission had three main objectives:

1. Perform a end-to-end test of the JEM-EUSO design in a near space environment

2. Measure the effective terrestrial UV background relevant for all space based fluorescence detectors (a discussion can be found in [7])

3. Detect UV light from above including laser tracks for the first time.

The latter is an important milestone for space based fluorescence measurements. The detector was flown as a stratospheric balloon payload during the moonless night of the 24th/25th of August 2014. It was launched from the Timmins (Canada) stratospheric balloon launch facility. A essential part of the mission was a 2.5 hour underflight using a helicopter equipped with three UV light sources. The light sources were used to perform a inflight calibration and to test the instrument's detection capabilities. The instrument and mission have been reported elsewhere [8].
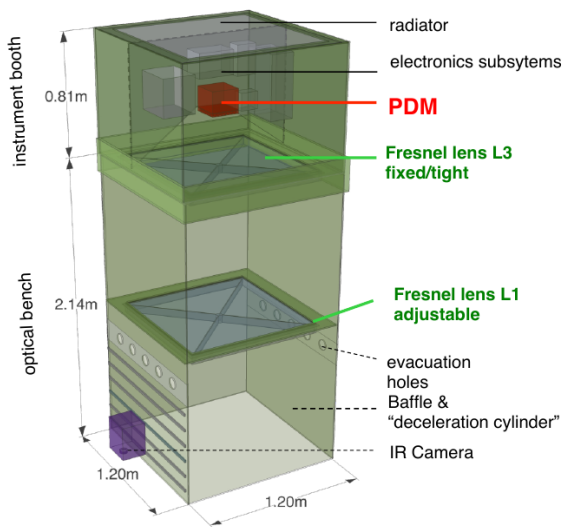
Figure 1: left: schematic of the flown EUSO-Balloon detector [9]; right: the actual detector

2. Detector

An overview of the detector is shown in fig. 1 and table 1 list its key properties. The instrument is a high speed UV camera designed to measure the fluorescence light of cosmic ray air showers. The two main components are the optical bench and the instrument booth. The optical bench contains two Fresnel lenses with an aperture of $1\,m^2$ to focus the light arriving at the instrument's aperture onto the Photo Detection Module (PDM) of EUSO-Balloon. The point spread function (PSF) of the optics was defined as the FWHM of a two-dimensional Gaussian fit the focal point. For EUSO-Balloon this gives 9.0 ± 0.2 mm or 3×3 pixels corresponding to $0.7° \times 0.7°$. EUSO-Balloon had a field of view of $\pm 11\,°$. A detailed description the the performance of the optical system is given in [10].

The PDM (see fig. 2) is made of 36 Hamamatsu M64 Multi-Anode Photomultiplier Tubes (MAPMT) each containing 64 anodes (2304 pixels in total) capable of single photoelectron counting. The Schott BG3 optical filter leads to a detection band of 290 to 430 nm. The integration time of the detector is $2.5\,\mu s$ (equivalent to 1 gate time unit, GTU). One event trigger causes 128 GTUs of data to be collected from all pixels. The trigger rate during the flight was 20 Hz, set by an internal clock.

3. Laser system and motivation

To evaluate the detectors capability to measure light from an extensive air shower (EAS) and to perform an in-flight calibration, three light sources were mounted to a helicopter that flew under the balloon (see fig. 3). An illustration of the underflight arrangement is shown in figure 4. The three light sources were: a UV-LED, a Xe-Flashlamp, and a UV-laser. Light is scattered isotropically out of a randomly polarized, pulsed laser beam when shot into the atmosphere. This light can be recorded by a fluorescence telescope used to look for cosmic rays. Both, air shower and laser,
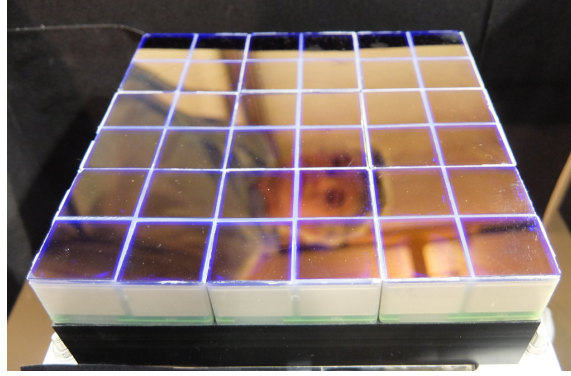
Figure 2: Top view picture of the PDM with filters attached

	Specification	Notes
Telescope Optics	2 1 m^2 Fresnel Lenses	PMMA
Field of View	11°×11°	
Number of Pixels	2304 (48×48)	36 64 ch. MAPMTs
MAPMT	R11265-113-M64-MOD2	Hamamatsu
UV Filter	BG-3, 2 mm thick	1 per MAPMT
Read Out	DC coupled	40 MHz double pulse resolution
Time Bin Duration	2.5 μs integration	event packet = 128 bins (320 μs)
Flight CPU	Atom N270 1.6 GHz processor	Intel
Telemetry	≈1.3 Mbits/s	NOSYCA CNES
Power Consumption	70 W	
Detector Weight	467 kg	
Balloon	0.4×10^6 m^3)	helium
Nominal Float Height	38300 m	
Launch	August 25 00:53 UTC 2017	48.57 lat 81.38 long
Flight Duration	8 hours	

Table 1: Specifications of EUSO-Balloon and 2014 mission.

Figure 3: The light sources were mounted on a Bell 212 helicopter. This dual turbine model was used because it satisfied various rules for night flight in Canada.
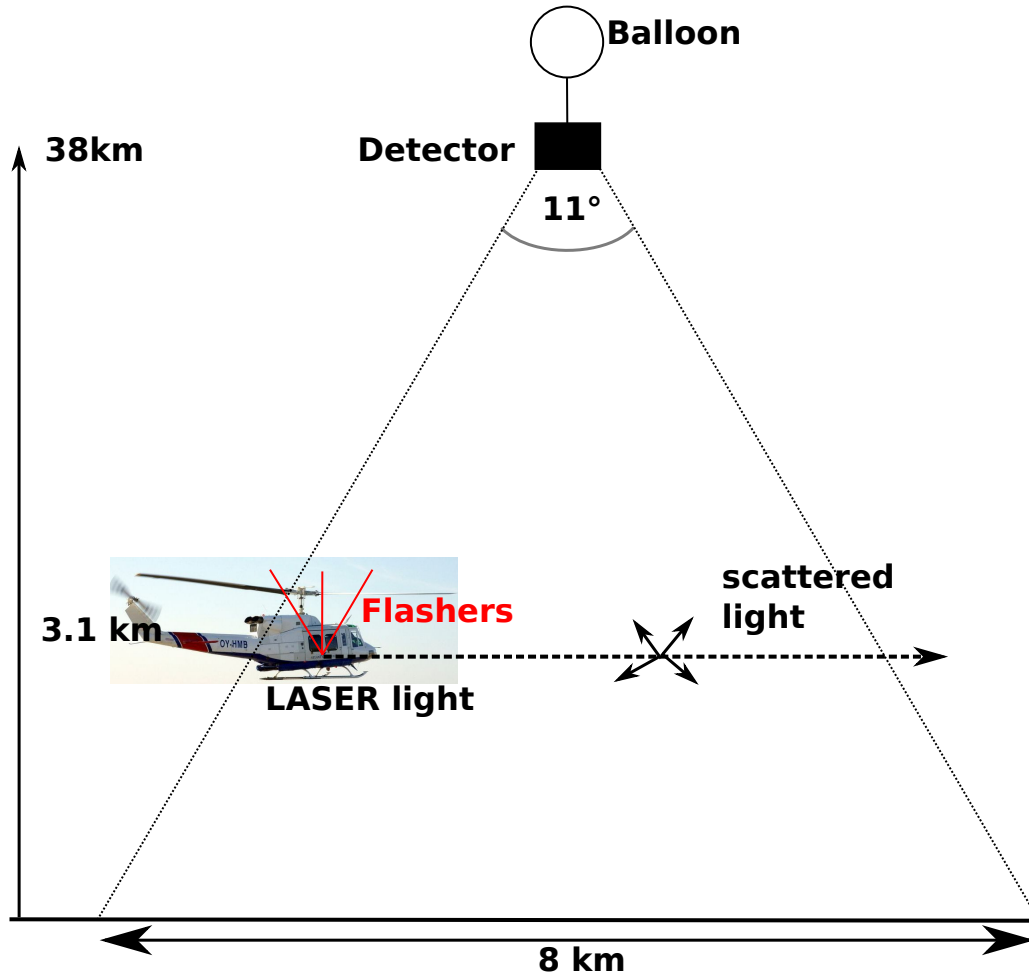
Figure 4: Sketch of the helicopter underflight

produce a track moving with the speed of light in the detector. Unlike showers it is possible to set the laser energy and direction and repeat the measurement when ever needed. This makes a laser a perfect test beam for fluorescence cosmic ray detectors. A more detailed study is presented in [11]. This paper will focus on the laser as a light source. Additional details of the LED and the flash-lamp can be found in [13]. The laser used was a Quantel CFR-Ultra [14] YAG-laser with frequency tripling to 355 nm. This wavelength was chosen because it is in the middle of the fluorescence spectrum (see fig. 5). Its maximum energy is 18 mJ with a 7 ns pulse width. The optical setup is shown in fig. 6. Harmonic separators are used to archive a spectral purity of more than 99.9%. A $3\times$ beam expander reduces the divergence to less than $0.04°$. The beam splitter divers 5% of the primary beam onto a pyroelectric probe [15] that measures the relative energy for every discharge. The depolarizing optic is used to randomly polarize the laser beam. This way the the scattering out of the beam in air would be symmetric in the azimuth angle about the beam axis.

The beam characteristics are listed in table 2. The laser system was calibrated before and after the flight by measuring the ratio between the monitor energy probe and a second energy probe placed temporarily in the beam downstream of all optics. The difference between this calibration
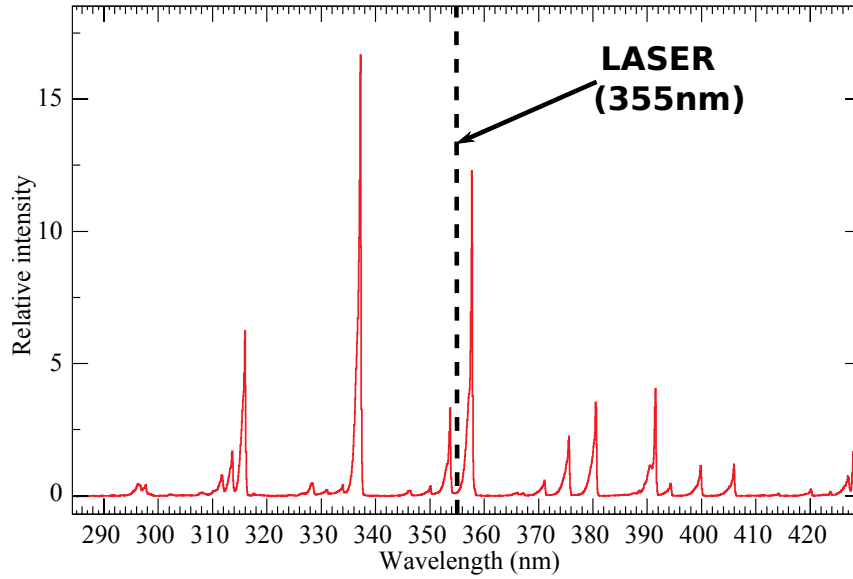
Figure 5: The wavelength of the laser (355 nm) is indicated on the fluorescence spectrum of electrons in air [12].
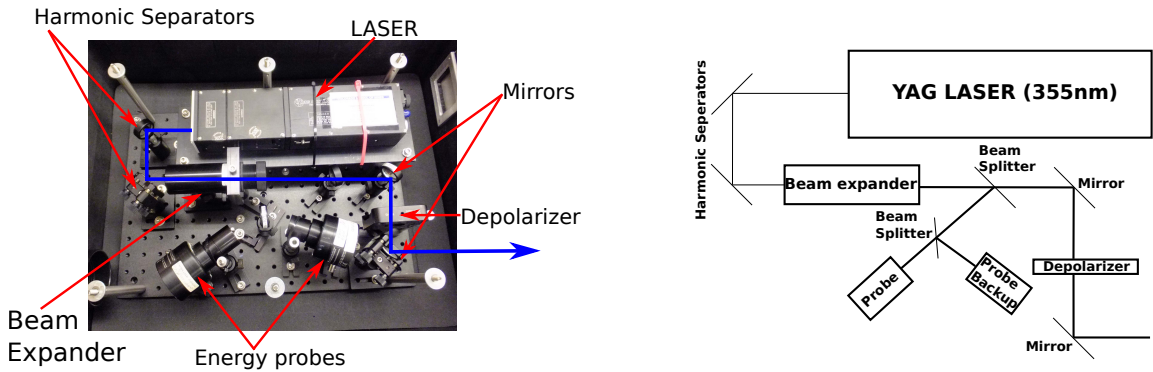

Figure 6: Left: The UV-laser system that was flown in the helicopter. The thick blue line indicates the beam path. Right: Schematic of the UV-laser system

factor measured before and after the flight was 1.2 %. The laser system is controlled by a Single

wavelength	355 nm	divergence	$< 0.04\,^\circ$
relative energy calibration	$> 2\%$	beam halo	$< 0.5\%$
absolute energy calibration	$> 4.5\%$	spectral purity	$> 99.9\%$
overall stability	1.2%	beam pointing direction	vertical: 3°
depolarization	$< 4\%$		horizontal: 1°
absolute timing accuracy	$\pm 20\,\text{ns}$		

Table 2: Laser beam characteristics

Board Computer(SBC). The key component of the SBC is the "GPSY2" module [16]. It contains an on-board GPS receiver, two 5 V outputs, and one analogue input, which triggers the readout of all components. The timing accuracy is 100 ns. The SBC was used to trigger the light sources in a specific order (1. LED, 2. Laser, 3. Xe-Flasher). The sequence was timed so that light from the three sources could reach the detector in the same 128 GTU readout window.

The system was mounted within a Bell 212 helicopter. The laser beam was fired through a partially open door, perpendicular to the body of the helicopter and horizontally when the helicopter was flying level.

4. Flight summary

The balloon was launched on the 25th of August 2014 at 00:53 UTC and reached a float altitude of approximately 38 km after an ascent of 2h 50m. After 4h 40m at float altitude the payload was released from the balloon (8:20 UTC) and landed 39 minutes later in a lake. The trajectories of the balloon and the helicopter are shown in fig. 7 and the timeline of the mission is shown in figure 8. The flight path of the helicopter is plotted in red in figure 7.

For the underflight the helicopter arrived from Ottawa (helicopter base, 550 km from Timmins) on the evening of the launch. After refueling in Timmins, it followed the balloon using a GPS tracking system. The tracking system consisted of a GPS module and a beacon mounted on the balloon and a receiver on board of the helicopter [13]. At 03:31 UTC the helicopter entered the FoV of the detector and the light sources were turned on. At the height of the helicopter the FoV of the detector is 8 by 8 kilometers. To trigger pixels across the whole PDM, the pilots flew circular loops with a radius smaller than 4 km centered on the latitude/longitude of the balloon while the laser was pointing towards the center of the circles. The sources were fired $\sim$ 150000 times in 2.28 hours.
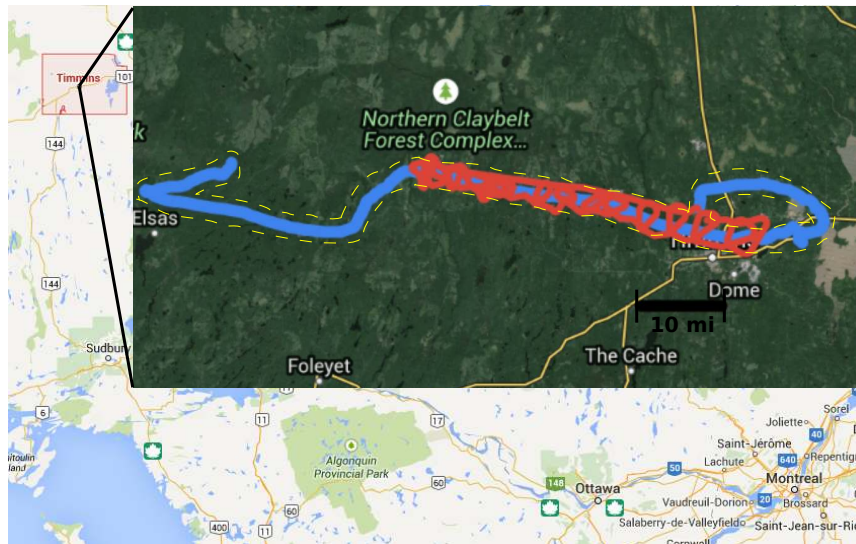

Figure 7: The thick blue line shows the flight path of the balloon. The yellow dashed line is the approximate FoV. The red line (loops) shows the flight pattern of the helicopter while the light sources were firing (*created with Google maps*).
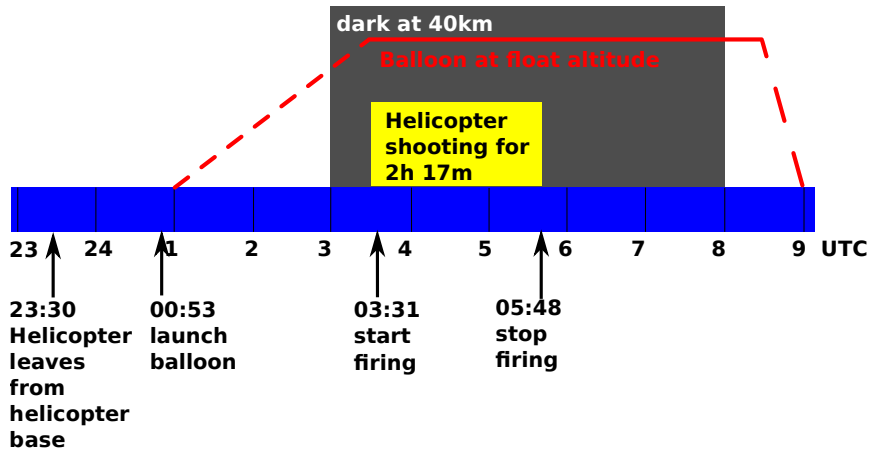
Figure 8: Timeline of the balloon and helicopter mission. The dashed line indicates the balloon.

5. Data collection and example events

The laser energy was switched every two minutes between ∼15 mJ and ∼10 mJ. The nominal laser energy correspond to an EAS energy of about 100 EeV. A 19 Hz repetition rate was chosen to obtain a chance overlap at regular intervals between the 20 Hz readout of the balloon and the laser. This arrangement worked around a problem with the clock synchronization between the two systems, possibly caused by a faulty GPS antenna on the balloon. A 20 Hz readout and a 19 Hz firing frequency result in a chance overlap every 380th shot. The laser was fired this way for 105260 times. That gives 277 overlaps. Out of these we were able to reconstruct 196. One reason for the lower number could be obstruction by clouds between the laser and the detector or positioning of the laser. The average energy of the shots, measured at the laser system, as a function of time can be seen in figure 9. The energy is decreasing over time due to heating of the laser. The laser shots that were recorded by EUSO-balloon are superimposed. Most of the events were recorded when there were no clouds between the laser and the balloon.

An example of an recorded laser track can be found in figure 10.

6. Analysis of laser events

6.1 Track identification

A track is a set of triggered pixels of multiple GTUs. To identify tracks in the externaly triggered data a two step pseudo-trigger was implemented in the offline data analysis. The first level is a simple threshold trigger which selects events in which at least N pixels are above background. If an event passes this simple trigger, it will be processed by the second level trigger which is looking for tracks. To determine if the set of triggered pixels form a track two algorithms are available: nearest neighbor, linear time fit. Both algorithm use cluster of triggered pixels. The first adds a cluster to the track selection if it is neighboring another cluster in space and time. In case multiple tracks are found by this algorithm, the longest one is chosen. This method finds 205 tracks in the data. The second algorithm is more complex. It performs a linear time fit on the clusters to identify
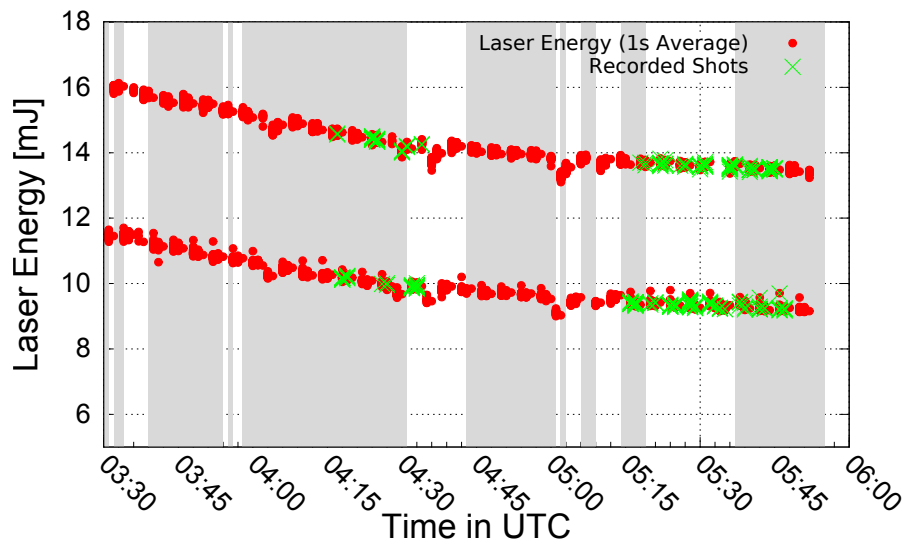
Figure 9: Red dots: Energy of all fired laser shots averaged over 19 shots (1 s). Green Xs: Shots recorded by EUSO-balloon. Grey regions indicate the likely presence of clouds.
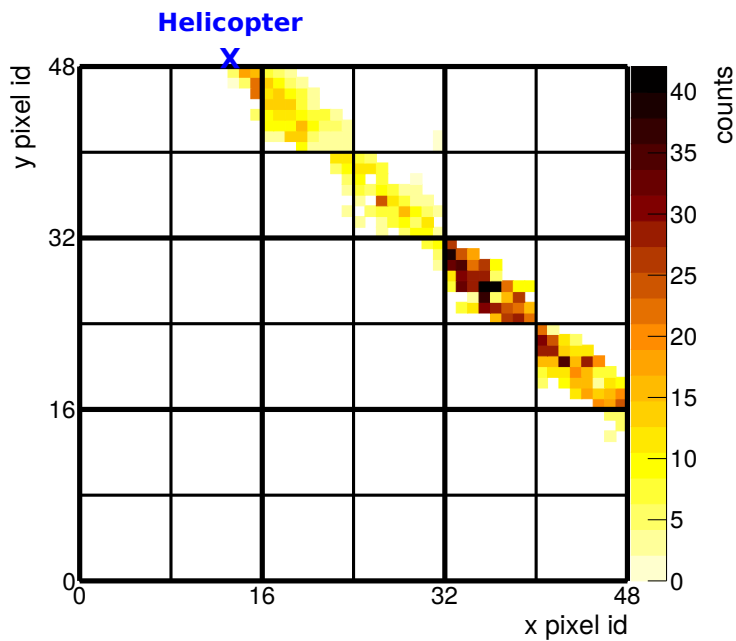

Figure 10: Laser track in the PDM at 05:29:25 UTC. Color represents the FADC counts. The blue X is the helicopter position at this time.

tracks in the data. 205 tracks are found with this algorithm as well. This one is used for the here presented work.

6.2 Algorithm for geometric reconstruction

In this section we explain the algorithm use to determine the geometry of the laser track. The

analysis follows two major steps. First, the pointing direction of the selected pixels is used to find the Shower Detector Plane (SDP) (Fig. 11). The SDP is given by the location of the detector and the line of the shower axis. The norm vector of the SDP, **SDP** is given by the pointing direction of the triggered pixels and weighted by their count.

$$\mathbf{S\hat{D}P} = \frac{1}{\sqrt{(\sum_{i;j>i} C_i C_j \mathbf{n}_i \times \mathbf{n}_j)^2}} \sum_{i;j>i} C_i C_j \mathbf{n}_i \times \mathbf{n}_j, \tag{6.1}$$

where C_i, n_i being, respectively, the charge and a unit vector along the pointing direction of the ith pixel in the track. **u** is a unit vector lying in the SDP that is pointing in the horizontal direction.

To reconstruct the direction of the event in the SDP, a trial nominal direction is estimated. Then the expected time for the signal to reach the detector is calculated for each pixel based on the region of the event axis to which it points (see Eq. 6.2). The difference between the expected and the observed time is compared and the parameters are adjusted to minimize time differences across the camera using the χ^2 minimization method. The geometry with the minimum difference is used to reconstruct the shower axis. The distance of closest approach, R_P, and the angle from horizontal to R_P, ψ_0 are the two parameters describing the axis. The arrival time at the ith pixel is given by

$$t_{i,expected} = T_0 + \frac{R_P}{c} \tan\left(\frac{\pi}{4} + \frac{\psi_0 - \psi_i}{2}\right) \tag{6.2}$$

where $\psi_i = \mathrm{acos}(\mathbf{u} \cdot \mathbf{n}_i)$ is the pointing direction of each participating pixel in the SDP. T_0 is the time when the shower front reaches R_P. If the change in angular speed $d\psi/dt$ is small over the observed track length (low curvature in time vs. angle), the uncertainties in the 3 parameter fit can be large.
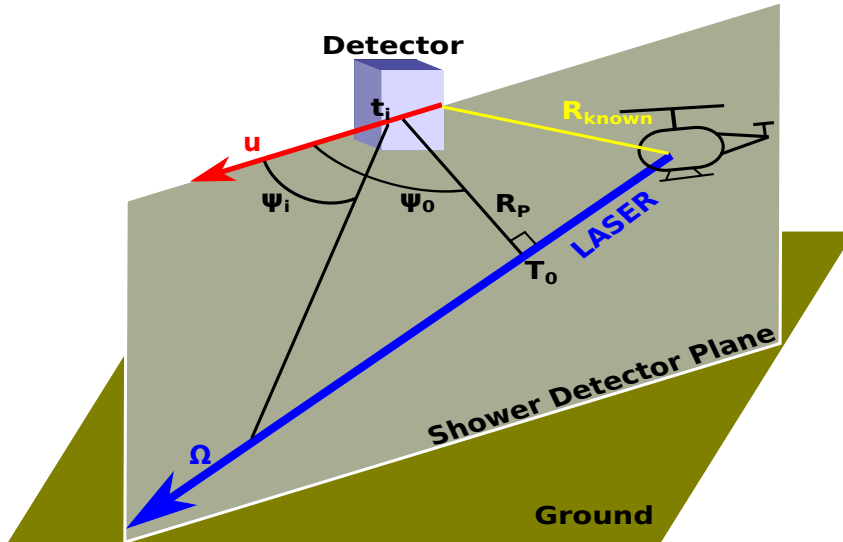

Figure 11: Illustration of the geometrical direction reconstruction of the laser tracks fired from the helicopter using the observables from the balloon.

A constraint fit can be performed using a known position along the track. For example the source position. This reduces the number of parameters in Eq.(6.2) from 3 to 2 (T_0 and ψ_0) given by

$$t_{i,ex} = T_0 + \frac{R_{known}}{c} \cdot \cos(\psi_{known} - \psi_0) \cdot \tan(\frac{\pi}{4} - \frac{\psi_i - \psi_0}{2}) \tag{6.3}$$

where R_{known} is the distance between the detector and the known source point (in our case, the helicopter position), and ψ_{known} is the angle between the horizontal and the known source point. This angle is calculated based on the GPS positions of the detector and the helicopter.
Finally, the laser reconstructed direction is given by

$$\mathbf{\Omega} = \sin(\psi_0)\hat{\mathbf{u}} - \cos(\psi_0)\left(\hat{\mathbf{u}} \times \hat{\mathbf{SDP}}\right), \tag{6.4}$$

where, the vector $\hat{\mathbf{u}}$ is contained in the SDP. It is therefore, perpendicular to the $\hat{\mathbf{SDP}}$, and can be simply taken as $\mathbf{u} = (\hat{\mathbf{SDP}}_y, -\hat{\mathbf{SDP}}_x, 0)$.

6.3 Results of the direction reconstruction

The laser tracks from the underflight have been analyzed to reconstruct the laser direction relative to the detector. An example track is shown in fig. 12 with the corresponding two-parameter timing fit (see equation 6.3). In this case, the fit was constrained using the position of the helicopter.
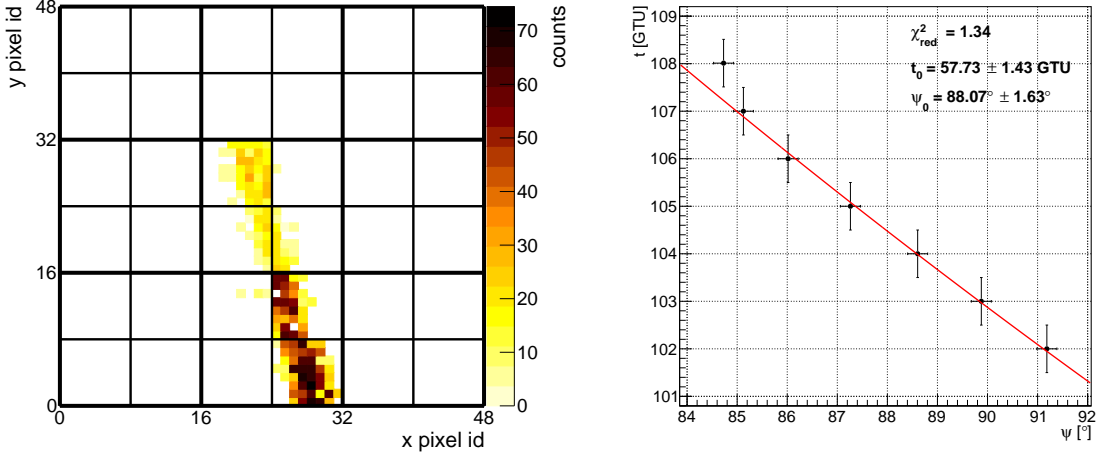
(a) laser track in the PDM. Colour represents the relative charge

(b) Timing profile of a laser event with constant 0.5 GTU timing error.

Figure 12: Example laser track at 05:40:24 UTC with corresponding time profile and fit.

The instrument captured 205 laser track candidates. To ensure that the candidate is indeed a track and not a false positive of the track finding algorithm, we required a track length of at least 4 GTUs which corresponds to at least 2 degrees of freedom in our fit. Since the tracks were nominally horizontal, the track length is directly related to the observation duration expressed as
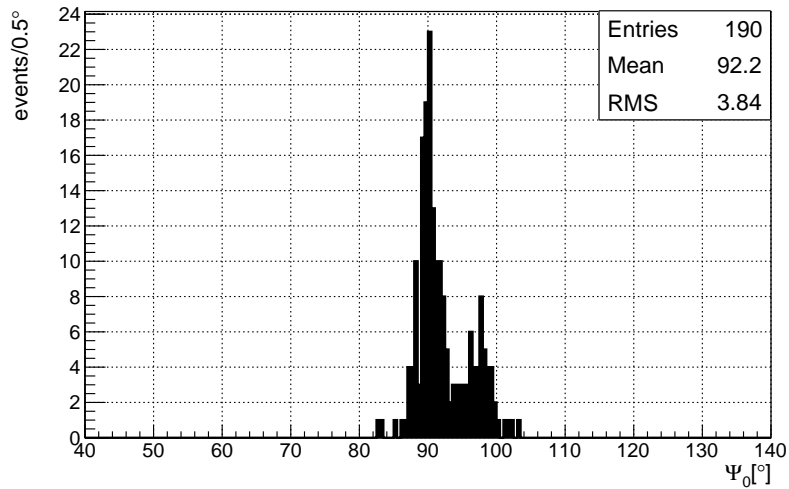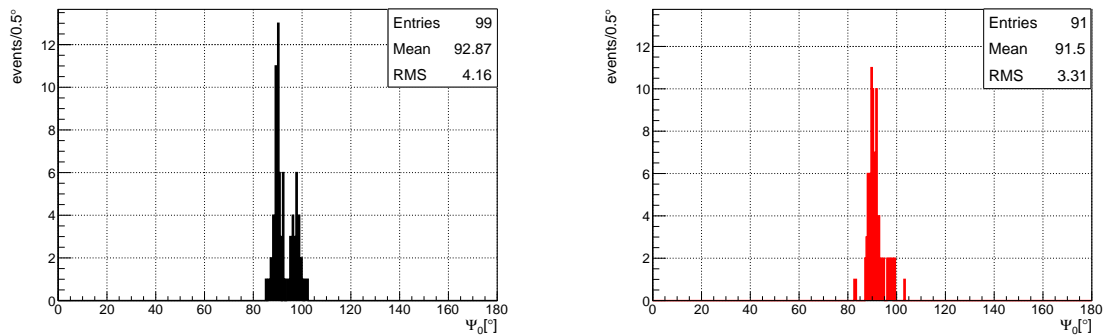
Figure 13: Zenith angle reconstruction of the helicopter laser shots with the 2 parameter fit method including only tracks with 4GTU or more.

(a) 2 Parameter reconstruction for an average laser energy of $10\,\mathrm{mJ}$(low setting)

(b) 2 Parameter reconstruction for an average laser energy of $15\,\mathrm{mJ}$(high setting)

Figure 14: Zenith angle reconstruction of the helicopter laser shots with the 2 parameter fit method split by laser energy. The minimum track duration is 4 GTUs.

the number of GTUs. This criteria reduces the number of tracks to 190. The reconstructed tilt angle is histogrammed in fig. 13.

The distribution of the 190 reconstructible events has a mean tilt angle of $92.2\,^\circ$ with a root mean square (RMS) of $3.8\,^\circ$. The two populations visible are related to the two energy settings used for the laser. While the lower energy setting is contributing to both population the higher setting only contributes to the population centered around $90\,^\circ$. A possible explanation for this behavior is saturation of the camera which shifts the weight of the timing fit. The result of splitting the dataset into high and low energy setting is shown in fig. 14

The expected mean value of the distribution should be slightly above $90\,^\circ$. The reason for that is the laser was mounted to produce horizontal tracks (meaning a zenith angle of $90\,^\circ$). We expect a slightly higher value, laser pointing to the ground, taking the flight pattern of the helicopter into

account. The helicopter was slightly turned sideways towards the ground by approximately 1-2 $^\circ$ to fly a circular pattern. The estimation of the bank angle uses the velocity of the helicopter and the assumption of truly circular flight pattern ($\theta = \arcsin(v^2/(R \cdot g))$). The velocity of the helicopter was recorded via on board GPS with 1 Hz as well as the position. Using the position information it is possible to fit circles to the flight pattern and obtain an approximated radius for segments of the flight. The shift to the higher mean value is under investigation and could perhaps be improved with a more accurate pixel pointing map.

7. Conclusion

The 2014 EUSO-Balloon flight made the first measurements of optical tracks by a fluorescence detetcor looking down on the atmosphere. The measurement required coordinating successfully the logistics of a balloon launch, a nighttime helicopter flight, on board laser and light sources, and gps tracking. The laser tracks are simulating the signal of an EAS, proving the capability of EUSO-Balloon to observe such a signal.

Although the laser was too bright to perform an energy reconstruction (pixel were saturated), the beam direction was reconstructed relative to the detector. In the reconstruction it was assumed that the track is moving with the speed of light. The fact that the reconstructed angles are reasonable, insures that this assumption is true. The direction of the tracks could be reconstructed with a precision of $\pm 3.8^\circ$. The spread is less for the high energy setting of the laser than for the lower one. We note that the offset of $\sim 2^\circ$ below horizontal is consistent with the estimated average tilt of the circling helicopter.

There are various reasons for this angular resolution. EUSO-Balloon is a prototype instrument designed mainly to demonstrate the JEM-EUSO proof of principle. The detector was equipped with only two of the three Fresnel lenses in the original design for the optics, leading to a point spread function of around 9 pixel ($\simeq 0.7^\circ$). In addition, the PDM had dead spots and only 30% of the PDM were properly calibrated. The 2.5 μs resolution was too large for a reconstruction angular resolution within a few degrees at a short distance between the helicopter and the balloon (35 km). This resolution does not represent the final resolution of the JEM-EUSO instrument. The distance between the detector and the shower will be around 10 times larger resolving the time resolution issue. The discovered issues during the mission lead to an upgrade in the electronics used in the subsequent mission: EUSO-SPB1 [5]. Furthermore the experience will play an important roll for the planned mission of EUSO-SPB2 [**?**].

References

[1] M. Casolino for the JEM-EUSO Collaboration, *The EUSO missions to study UHECR from space: status and perspectives in Proc 35th ICRC*, (Busan), PoS(ICRC2017)370 (2017).

[2] P. Klimov et al., [JEM-EUSO Collaboration], *Status of the KLYPVE-EUSO detector for EECR in Proc. 35th ICRC*, (Busan), PoS(ICRC2017)412 (2017).

[3] A. Olinto et al., *POEMMA: Probe Of Extreme Multi-Messenger Astrophysics in Proc. 35th ICRC*, (Busan), PoS(ICRC2017)542 (2017).

[4] L.W. Piotrowski et al.,[JEM-EUSO Collaboration], *The EUSO-TA detector: status and performance in Proc. 35th ICRC*, (Busan), PoS(ICRC2017)374 (2017).

[5] L. Wiencke et al., [JEM-EUSO Collaboration], *EUSO-SPB1 Mission and Science in Proc. 35th ICRC*, (Busan), PoS(ICRC2017)1097 (2017).

[6] M. Ricci et al., [JEM-EUSO Collaboration], *Mini-EUSO: a pathfinder for JEM-EUSO to measure Earth's UV background from the ISS in Proc. 34th ICRC*, (The Hague), PoS(ICRC2015)599 (2015).

[7] S. Mackovjak et al., [JEM-EUSO Collaboration], *Night Time Measurement of the UV Background by EUSO-Balloon in Proc. 34th ICRC*, (The Hague), PoS(ICRC2015)685 (2015).

[8] P. von Ballmoos et al., [JEM-EUSO Collaboration], *General overview of EUSO-balloon mission in Proc. 34th ICRC*, (The Hague), PoS(ICRC2015)322 (2015)

[9] P. von Ballmoos et al., [JEM-EUSO Collaboration], *EUSO-balloon : A pathfinder for observing uhecr's from space in Proc. 33th ICRC*, (Rio de Janeiro), (ICRC2013)1171 (2013).

[10] C. Catalano et al., [JEM-EUSO Collaboration], *Performance of the EUSO-Balloon optics in Proc. 34th ICRC*, (The Hague), PoS(ICRC2015)622 (2015).

[11] C. Medina, PhD Thesis, *The Central Laser Facility at the Pierre Auger Observatory. Studies of the Atmospheric Vertical Aerosol Optical Depth and Other Applications to Comic Ray Mesurements*, Colorado School of Mines, (2017).

[12] M. Ave et al., [AIRFLY], Astropart. Phys. **28**, 41 (2007).

[13] J. Adams et al., [JEM-EUSO Collaboration], *The calibration of EUSO-balloon using airborne light sources mounted to a helicopter in Proc. 34th ICRC*, (The Hague), PoS(ICRC2015)580 (2015).

[14] Quantel-laser, http://www.quantel-laser.com.

[15] Laser Probe Inc., http://www.laserprobeinc.com/.

[16] J. Smith, J. Thomas, S. Thomas, and L. Wiencke, *System and method for precise absolute time event generation and capture*, US Patent 7,975,160 (2011).

[17] J. Adams et al., *White paper on EUSO-SPB2* arXiv:1703.04513v2.